

AD-A106 135

STANFORD UNIV CA DEPT OF CHEMISTRY

F/G 7/5

UNIMOLECULAR FRAGMENTATION KINETICS BY MULTIPHOTON IONIZATION, (U)

APR 81 D PROCH, D M RIDER, R N ZARE

DAAG29-80-K-0097

UNCLASSIFIED

ARO-17745.1-C

NL

[ 10 ]

10/10/80



END

DATE

FILED

11 81

DTIC

AD A106135

REPRINTED FROM:

# CHEMICAL PHYSICS LETTERS

ARL 17745.1-C

2

Volume 81, No. 3, 1 August 1981

UNIMOLECULAR FRAGMENTATION KINETICS BY MULTIPHOTON IONIZATION\*

D. PROCH<sup>†</sup>, D.M. RIDER and R.N. ZARE

*Department of Chemistry, Stanford University, Stanford, California 94305, USA*

pp. 430-434

DTIC FILE COPY



NORTH-HOLLAND PUBLISHING COMPANY - AMSTERDAM

DTIC  
ELECTE  
OCT 27 1981  
S A D

81 10 20

Unclassified

SECURITY CLASSIFICATION OF THIS PAGE (When Data Entered)

| REPORT DOCUMENTATION PAGE   |  | READ INSTRUCTIONS<br>BEFORE COMPLETING FORM                           |
|---|--|---|
| 1. REPORT NUMBER<br>17745-1-C   | 2. GOVT ACCESSION NO.<br>AD-A106135<br>N/A | 3. RECIPIENT'S CATALOG NUMBER<br>N/A                                  |
| 4. TITLE (and Subtitle)<br>Unimolecular Fragmentation Kinetics by<br>Multiphoton Ionization,                                |  | 5. TYPE OF REPORT & PERIOD COVERED<br>Reprint                         |
| 6. AUTHOR(s)<br>D. Proch<br>D. M. Rider<br>R. N. Zare   |  | 6. PERFORMING ORG. REPORT NUMBER<br>N/A                               |
| 7. PERFORMING ORGANIZATION NAME AND ADDRESS<br>Stanford University<br>Stanford, CA 94305                                    |  | 8. CONTRACT OR GRANT NUMBER(s)<br>DAAG29-80-K-0097,<br>VAFOSR-81-0053 |
| 9. CONTROLLING OFFICE NAME AND ADDRESS<br>U. S. Army Research Office<br>P. O. Box 12211<br>Research Triangle Park, NC 27709 |  | 10. PROGRAM ELEMENT, PROJECT, TASK<br>AREA & WORK UNIT NUMBERS<br>N/A |
| 11. MONITORING AGENCY NAME & ADDRESS (if different from Controlling Office)   |  | 12. REPORT DATE<br>1 Aug 81   |
|   |  | 13. NUMBER OF PAGES<br>5  |
|   |  | 14. SECURITY CLASS. (of this report)<br>Unclassified                  |
|   |  | 15a. DECLASSIFICATION/DOWNGRADING<br>SCHEDULE                         |
| 16. DISTRIBUTION STATEMENT (of this Report)<br><br>Submitted for announcement only.   |  |   |
| 17. DISTRIBUTION STATEMENT (of the abstract entered in Block 20, if different from Report)                                  |  |   |
| 18. SUPPLEMENTARY NOTES   |  |   |
| 19. KEY WORDS (Continue on reverse side if necessary and identify by block number)  |  |   |
| 20. ABSTRACT (Continue on reverse side if necessary and identify by block number)   |  |   |

DD FORM 1 JAN 73 1473

EDITION OF 1 NOV 65 IS OBSOLETE

Unclassified

SECURITY CLASSIFICATION OF THIS PAGE (When Data Entered)

## UNIMOLECULAR FRAGMENTATION KINETICS BY MULTIPHOTON IONIZATION\*

D. PROCH<sup>†</sup>, D.M. RIDER and R.N. ZARE*Department of Chemistry, Stanford University, Stanford, California 94305, USA*

Received 20 April 1981

The multiphoton ionization spectrum of aniline and its perdeutero analog have been investigated for laser wavelengths 266–300 nm using a time-of-flight mass spectrometer. A broad, asymmetrically distorted peak at  $m/e = 66$  is interpreted to be the slow fragmentation of the parent ion,  $C_6H_7N^+ \rightarrow C_5H_6^+ + HCN$ ; its unimolecular decomposition rate is  $\approx 2 \times 10^6 \text{ s}^{-1}$ .

## 1. Introduction

Ever since Hipple et al. [1] identified that the diffuse peaks in a mass spectrum are caused by the decomposition of ions in the course of mass analysis, the importance of understanding unimolecular reactions of ions has been recognized. While electron impact mass spectrometry was the first method for observing these "metastable" ions, many new techniques have been developed to study this phenomenon. The most informative are those in which the reactant ions are created with a well-characterized distribution of internal energies and in which this distribution can be readily controlled. This usually calls for the use of vacuum ultraviolet (VUV) photoionization [2–4]. Unfortunately, the number of such studies is very limited because of the difficulty of producing and manipulating sufficiently intense tunable VUV radiation.

An alternative to one-photon VUV photoionization is multiphoton ionization (MPI) in which the absorption of more than one visible or near UV photon causes ionization [5]. The MPI technique has many advantages [6]. Because of the resonant enhancement provided by intermediate states, MPI can produce large numbers of ions with moderately intense laser sources [7]. Moreover, MPI studies only require conventional optics.

\* Research supported, in part, by the Air Force Office of Scientific Research under AFOSR-81-0053 and by the Army Research Office under DAAG-29-80-K-0097.

<sup>†</sup> Max Kade Fellow; on leave from Max-Planck-Institut für Quantenoptik, 8046 Garching, Federal Republic of Germany.

In this letter we present the first use of the MPI technique to study the unimolecular decomposition rates of ions. Aniline ( $C_6H_5NH_2$ ) is ionized by the multiphoton absorption of pulsed UV laser light (266–300 nm) and the resulting ions are mass analyzed by time of flight (TOF). We investigated the elimination of HCN from the aniline parent ion,  $C_6H_7N^+$ , to yield  $C_5H_6^+$ . Because of fragmentation during ion acceleration the daughter ion peak is asymmetrically distorted. Moreover, the extent of distortion changes with laser wavelength in a manner suggesting that the rate of fragmentation increases with photon energy.

## 2. Experimental

Fig. 1 shows a schematic diagram of the experimental apparatus. The unfocused output of a tunable frequency-doubled dye laser (Quanta Ray PDL-1) pumped by a Nd:YAG laser (Quanta Ray DCR-1A) is stopped down to a 1.75 mm diameter with two irises before passing through a TOF mass spectrometer. The wavelength range (266–300 nm) is obtained by frequency doubling the output of the dyes CS00, R590, R610 and kiton red (Exciton Chemical Co.). The pulse width of the laser is 5–7 ns. Power densities vary depending on the wavelength. Most spectra are recorded at the power level of 14 MW/cm<sup>2</sup>.

The TOF mass spectrometer was designed and built in this laboratory. The spectrometer utilizes a double-electric-field ion source [9] to accelerate the ions into

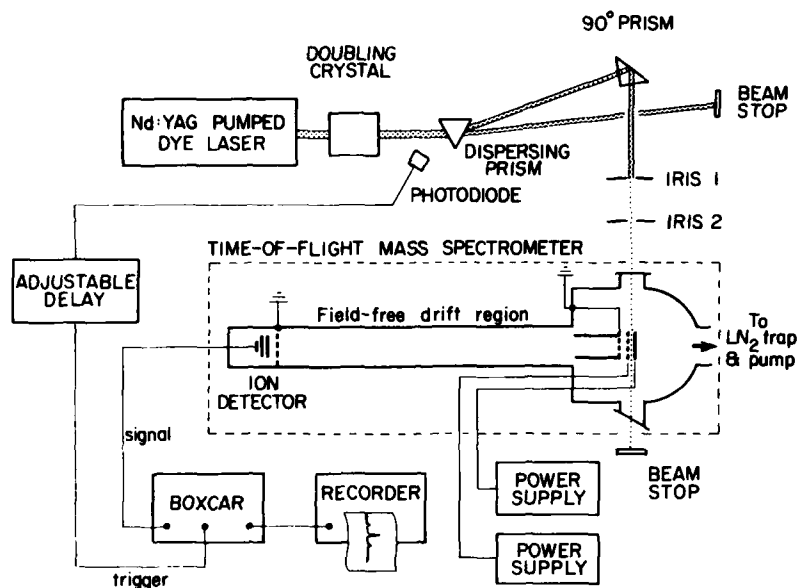


Fig. 1. Schematic diagram of the MPI time-of-flight mass spectrometer.

a 1.5 m field-free drift region. A relatively small electric field of 176 V/cm is applied in region I (shown in fig. 2). This low-field region serves to minimize the time-of-flight spread of ions of a single  $m/e$  ratio formed over the diameter of the laser beam. In region II there is a much higher electric field (4710 V/cm). The ions acquire most of their kinetic energy in this region. The resolution of the instrument is better than 200, i.e. the value of  $M/\Delta M$  at 10% of the peak height is greater than 200.

The ion bunches are detected and amplified by a microchannel plate electron multiplier (Varian model 8992-2). The signal from the multiplier is amplified and averaged with a boxcar integrator (Princeton Applied Research model 162 with model 165 plug-in). A photodiode triggers an adjustable delay generator which in turn triggers the boxcar. The output of the boxcar drives a stripchart recorder.

The TOF mass spectrometer is evacuated by a diffusion pump through a liquid-nitrogen-cooled cryotrap. The base pressure of the instrument is  $3 \times 10^{-8}$  Torr. Samples are admitted through a small tube with its orifice near the ionization region. The unfocused laser beam enters and exits through quartz windows in the vacuum chamber.

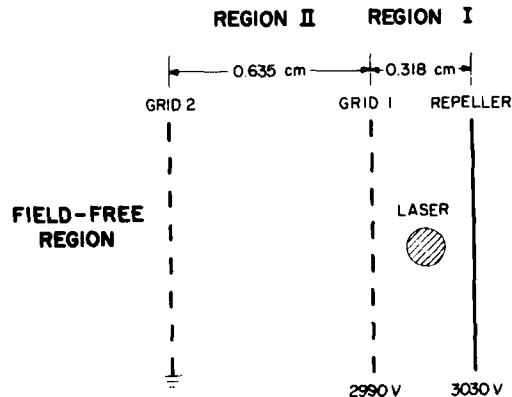


Fig. 2. Detailed drawing of the MPI TOF mass spectrometer ion source.

Reagent grade aniline (J.T. Baker Chemical Co.) and aniline- $d_7$  (98% D, Merck and Co.) are used without further purification. Both compounds are thoroughly degassed by several freeze-pump-thaw cycles before introduction into the TOF mass spectrometer. During a run, the partial pressure of aniline is  $1 \times 10^{-7}$  Torr, as measured by an ionization gauge.

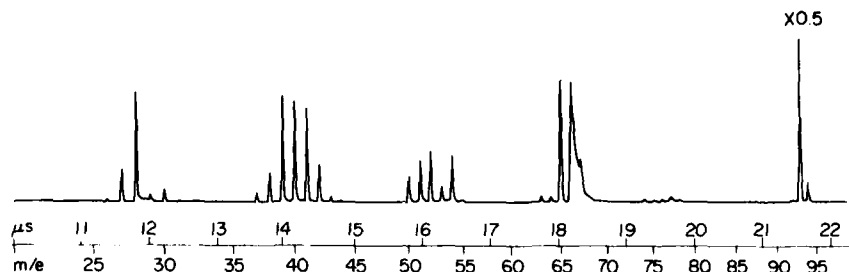


Fig. 3. MPI TOF mass spectrum of aniline: laser wavelength is 266 nm; laser power is 20 MW/cm<sup>2</sup>.

### 3. Results and discussion

#### 3.1. The TOF mass spectrum of aniline

Aniline is efficiently ionized by the absorption of two 266–300 nm photons because the process is resonantly enhanced by one-photon absorption to the  $^1B_2$  state [8]. The origin of the  $^1B_2$  state is at 293.9 nm [9] and the ionization potential of aniline is 8.32 eV [10]. As expected, the parent ion signal varies with the square of the laser power.

Fig. 3 shows the TOF MPI mass spectrum of aniline taken at a laser wavelength of 266 nm. The most intense feature is the parent ion ( $m/e = 93$  for  $C_6H_7N^+$ ) which is accompanied by the  $^{13}C^{12}C_5H_7N^+$  ion at  $m/e = 94$ . In addition, there is extensive fragmentation. The most intriguing aspect of this fragmentation pattern is the appearance of a distorted peak in the vicinity of  $m/e = 66$ .

It is well known that the extent of fragmentation in MPI depends strongly on laser power [7,8,12,13]. In the present study, only the parent ion of aniline appears at low power densities, while as the power density is increased, fragment ions appear. Fig. 3 is recorded under the latter condition at 20 MW/cm<sup>2</sup>.

Fig. 4 illustrates the TOF MPI mass spectrum in the region of  $m/e = 64$ –68 at several laser wavelengths. As the wavelength decreases the  $m/e = 66$  peak broadens and becomes asymmetric, trailing off toward higher masses (longer arrival times). This distortion begins to appear near 285 nm. Under the same condition that the  $m/e = 66$  peak broadens and distorts, the other peaks in the mass spectrum remain well resolved. Thus the appearance of the  $m/e = 66$  peak is not caused by limited

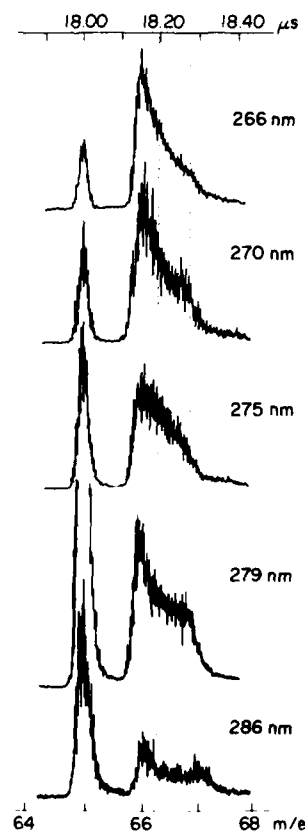


Fig. 4. Portion of the MPI TOF mass spectrum of aniline in the region of the  $m/e = 66$  peak as a function of laser wavelength. Each trace is recorded at the same laser power level (14 MW/cm<sup>2</sup>).

resolution of the TOF mass spectrometer. There are two possible isobaric components of the  $m/e = 66$  peak (neglecting  $^{13}\text{C}$  containing ions):  $\text{C}_5\text{H}_6^+$  and  $\text{C}_4\text{H}_4\text{N}^+$ . However, the equivalent ions of aniline- $d_7$ ,  $\text{C}_5\text{D}_6^+$  and  $\text{C}_4\text{D}_4\text{N}^+$ , are at  $m/e = 72$  and  $70$ , respectively. In the 266 nm MPI TOF mass spectrum of aniline- $d_7$   $m/e = 70$  is a well-resolved peak while  $m/e = 72$  is quite distorted. Hence we conclude that the formation of  $\text{C}_5\text{H}_6^+$  is the slow fragmentation step which causes the observed distortion. This is supported by the 70 eV electron impact mass spectrum [14] where  $\text{C}_5\text{H}_6^+$  contributes 93.4% and  $\text{C}_4\text{H}_4\text{N}^+$  6.6% at a nominal value of  $m/e = 66$ .

In the protonated compound the  $m/e = 66$  distorted peak shape has a contribution from  $m/e = 67$  ( $\text{C}_4\text{H}_5\text{N}^+$ ), which causes the appearance of a small peak or shoulder on the trailing portion of the  $m/e = 66$  peak. Often the presence of the  $m/e = 67$  peak is obscured by overlap with the  $m/e = 66$  peak, but TOF mass spectra taken at longer wavelengths clearly show its presence. Although this complicates the  $m/e = 66$  profile, the  $m/e = 67$  peak does not prevent us from determining qualitatively the distortion of the  $m/e = 66$  peak as a function of laser wavelength.

When  $\text{C}_5\text{H}_6^+$  is produced by electron impact ionization of aniline it is found to be formed from the metastable parent ion [14,15]. This implies that the rate of fragmentation to form  $\text{C}_5\text{H}_6^+$  is relatively slow compared to non-metastable fragments. It is the relatively slow rate of fragmentation that causes the  $\text{C}_5\text{H}_6^+$  to be a distorted peak in the MPI TOF mass spectrum. This can be ascertained by an analysis of ion trajectories in our TOF mass spectrometer.

Consider some parent and daughter ions that are formed at the center of region I (fig. 2) during the laser pulse. These two types of ions will be accelerated through regions I and II and enter the field-free region with the same kinetic energy but different velocities since they have unequal masses. Traversing the field-free region they will separate in time and space and be detected at a time difference that depends only on the ratio of the square roots of their masses. If, however, some of the parent ions fragment while they are being accelerated, the resulting daughter ions enter the field-free region with a velocity which is less than that of a daughter ion formed promptly in the center of region I but greater than that of the parent ion. The resulting daughter ion arrives at the detector at some intermediate time that

depends on the precise position of the fragmentation as well as the masses of the daughter and parent ions.

An ion gains most of its kinetic energy in region II and only a small fraction in region I. Decomposition of parent ions as they traverse region I produces fragments that are detected in an interval near the arrival time of a promptly formed fragment. Fragment ions formed in region II are detected in a time interval between those formed at grid 1 and the arrival time of the parent ion. Fragments formed in the field-free region arrive at the detector simultaneously with the parent ion and thus are indistinguishable from them. A fragment peak shape can thus have two detectable components. It is estimated for prompt  $m/e = 66$ –93 that residence times in regions I, II, and the field-free region are 400–500 ns, 115–130 ns, and 18–20  $\mu\text{s}$ , respectively. The major component is caused by fragmentation in region I. The component formed by fragmentation in region II contributes less because the parent ions spend less time in this region and the flight time of the fragments is distributed over a longer time interval. The transition from the first component to the second according to calculations is 90 ns after the arrival time of a promptly formed  $m/e = 66$  ion. It is observed as a sharp drop in intensity in fig. 4. The shape of component I is a measure of the relative number of fragments formed at each position in region I and is directly related to the fragmentation rate.

The unimolecular fragmentation rate of an ion depends on the amount of internal energy with which it is prepared. In the statistical case the rate increases rapidly with increasing internal energy [16]. Thus, with decreasing laser wavelength, more energy is deposited in the  $m/e = 93$  precursor and hence one would expect that the fragmentation rate increases. Inspection of fig. 4 shows this trend, as can readily be seen by the change of slope between the two vertical dotted lines. At the shortest wavelength, the slope is the steepest, corresponding to the most rapid rate of fragmentation.

The structure of the  $\text{C}_5\text{H}_6^+$  ion is uncertain. Occolowitz and White [17] argue that the  $\text{C}_5\text{H}_6^+$  ion from the electron impact ionization of aniline is linear and suggest it is the 3-penten-1-yne cation. In any case they determine an appearance potential from aniline for this ion to be 12.56 eV. This value is energetically equivalent to three photons at 298 nm. The distortion of the  $m/e = 66$  peak first appears near 285 nm, three photons of which are equivalent to 13.1 eV. In the wavelength

range studied we conclude that  $C_5H_6^+$  must be formed by the absorption of three photons. To the red of 285 nm the fragmentation rate may be too slow for the production of an appreciable number of  $C_5H_6^+$  ions in region I of the TOF mass spectrometer.

The calculation of a fragmentation rate from the data in fig. 4 is complicated by the mapping of the arrival times  $t$  of the daughter ion at the detector into formation times  $\tau$  of the daughter ion in the ion source. We assume that this unimolecular decomposition process is described by a single exponential. Then the number of daughter ions formed per unit time at time  $\tau$ ,  $D(\tau)$ , is related to the initial number of parent ions,  $P(0)$ , by

$$D(\tau) = k P(0) \exp(-k\tau), \quad (1)$$

where  $k$  is the rate constant. The ratio of the daughter ion formation rates, at two times  $\tau_1$  and  $\tau_2$  is given by

$$D(\tau_1)/D(\tau_2) = \exp[-k(\tau_1 - \tau_2)]. \quad (2)$$

We approximate the mapping of  $\Delta\tau$  in the ion source to  $\Delta t$  at the detector by a linear transformation. Then the corresponding signal ratio at the detector is

$$S(t_1)/S(t_2) = \exp[-k\alpha(t_1 - t_2)], \quad (3)$$

where under our operating conditions the scaling constant  $\alpha$  is  $\approx 5$ . We find from applying eq. (3) to the 266 nm signal shape of the  $C_5H_6^+$  ion shown in fig. 4 the fragmentation rate

$$k \approx 2 \times 10^6 \text{ s}^{-1}. \quad (4)$$

This value of  $k$  represents the phenomenological rate constant for the appearance of  $C_5H_6^+$  ions from aniline at this wavelength and power level. Because of the various approximations introduced in this simple analysis, eq. (4) may represent no better than an order of magnitude estimate. Computer simulations are in progress to refine this value of  $k$ . Preliminary results suggest that the uncertainty in  $k$  may be less than a factor of two.

The present study concerns the production of a metastable precursor to  $C_5H_6^+$  in the multiphoton ionization of aniline and the observation of its fragmenta-

tion rate as a function of laser wavelength. Multiphoton ionization can prepare parent ions with known internal energies and this can be accomplished with extreme spatial definition and temporal resolution. Thus, it would appear that MPI has a bright future for the study of ionic rearrangement/fragmentation kinetics.

## References

- [1] J.A. Hipple, R.E. Fox and E.U. Condon, Phys. Rev. 69 (1946) 347.
- [2] W.A. Chupka, in: Chemical spectroscopy and photochemistry in the vacuum ultraviolet, eds. C. Sandorfy, P.J. Ausloos and M.B. Robin (Reidel, Dordrecht, 1974) pp. 431-463.
- [3] A.S. Werner and T. Baer, J. Chem. Phys. 62 (1975) 2900.
- [4] H.M. Rosenstock, Intern. J. Mass Spectrom. Ion Phys. 20 (1976) 139.
- [5] P.M. Johnson, Accounts Chem. Res. 13 (1980) 20, and references therein.
- [6] V.S. Antonov and V.S. Letokhov, Appl. Phys. 24 (1981) 89.
- [7] D.M. Lubman, R. Naaman and R.N. Zare, J. Chem. Phys. 72 (1980) 3034.
- [8] J.H. Brophy and C.T. Rettner, Opt. Letters 4 (1979) 337; Chem. Phys. Letters 67 (1979) 351; C.T. Rettner and J.H. Brophy, Chem. Phys. 56 (1981) 53.
- [9] W.C. Wiley and I.H. McLaren, Rev. Sci. Instr. 26 (1955) 1150.
- [10] T. Cuitas, J.M. Hollas and G.H. Kirby, Mol. Phys. 19 (1970) 305.
- [11] H.M. Rosenstock, K. Draxl, B.W. Steiner and J.T. Herron, J. Phys. Chem. Ref. Data 6 (1977) 1-235, suppl. 1.
- [12] L. Zandee and R.B. Bernstein, J. Chem. Phys. 70 (1979) 2574; 71 (1979) 1359.
- [13] S. Rockwood, J.P. Reilly, K. Hohla and K.L. Kompa, Opt. Commun. 28 (1979) 175.
- [14] A.V. Robertson and C. Djerassi, J. Am. Chem. Soc. 90 (1968) 6992.
- [15] P.N. Rylander, S. Meyerson, E.L. Eliel and J.D. McCollum, J. Am. Chem. Soc. 85 (1963) 2723.
- [16] F.W. McLafferty, Interpretation of mass spectra (Benjamin, New York, 1973).
- [17] J.L. Occolowitz and G.L. White, Australian J. Chem. 21 (1968) 997.

|                    |   |
|--------------------|---|
| Accession For      | <input checked="" type="checkbox"/> <input type="checkbox"/> <input type="checkbox"/> |
| NTIS GRA&I         |   |
| DTIC TAB           |   |
| Unannounced        |   |
| Justification      |   |
| By                 | 14/73   |
| Distribution/      | unclassified  |
| Availability Codes |   |
| Avail and/or       |   |
| Dist Special       |   |
|                    | A 21  |



ATE  
LMED  
— 8